Data Assimilation

Observation Impact on the Short Range Forecast

C. Cardinali

Research Department

June 2013

Series: ECMWF Lecture Notes

A full list of ECMWF Publications can be found on our web site under:
http://www.ecmwf.int/publications/

Contact: library@ecmwf.int

European Centre for Medium-Range Weather Forecasts
Shinfield Park, Reading, RG2 9AX, England

Abstract

The concept and the use of the forecast error sensitivity to observations for diagnostic purposes are illustrated in this paper. The tool computes the contribution of all observations to the forecast error: a positive contribution is associated with forecast error increase and a negative contribution with forecast error decrease. The forecast range investigated is 24 hour. It can be seen that globally, the assimilated observations decrease the forecast error; locally however also poor performance can be found. The forecast deterioration can be related either to the data quality or to the data assimilation and forecast system. The data impact on the forecast is spatially and also temporally variable. It depends on atmospheric regimes, which may be well or not well represented by the model or by the data. An example of a routine diagnostic assessment of observational impact on the short-range forecast performance is shown. The example also illustrates the tools flexibility to represent different degrees of detail of forecast improvement or deterioration.

1 Introduction

The ECMWF four-dimensional variational system (4D-Var, Rabier *et al.* 2000) handles a large variety of both space and surface-based meteorological observations (more than 30 million a day) and combines the observations with the prior (or background) information on the atmospheric state. A comprehensive linearized and non-linear forecast model is used, counting 10^8 the order of degrees of freedom.

The assessment of the observational contribution to analysis (Cardinali *et al.* 2004, Chapnick *et al.* 2004, Lupu *et al.* 2011) and forecast is among the most challenging diagnostics in data assimilation and numerical weather prediction. For the forecast, the assessment of the forecast performance can be achieved by adjoint-based observation sensitivity techniques that characterize the forecast impact of every measurement (Baker and Daley 2000, Langland and Baker 2004, Cardinali and Buizza, 2004, Morneau *et al.*, 2006, Xu and Langlang, 2006, Zhu and Gelaro 2008, Cardinali 2009). The technique computes the variation in the forecast error due to the assimilated data. In particular, the forecast error is measured by a scalar function of the model parameters, namely wind, temperature, humidity and surface pressure that are more or less directly related to the observable quantities.

In general, the adjoint methodology can be used to estimate the sensitivity measure with respect to any assimilation system parameter of importance. For example, Daescu (2008) derived a sensitivity equation of an unconstrained variational data assimilation system from the first-order necessary condition with respect to the main input parameters: observation, background, and observation and background error covariance matrices.

The forecast sensitivity to observation technique (FSO) is complementary to the Observing System Experiments (OSEs) that have been the traditional tool for estimating data impact in a forecasting system (Bouttier and Kelly, 2001; English *et al.*, 2004; Lord et al., 2004; Kelly 2007 and Radnoti *et al.*, 2010 and 2012). Very important is the use of OSEs in complement to FSO to highlight the contribution e.g. of a particular data set and to address the causes of degradation or improvement which FSO measures.

The main differences between adjoint-based and OSE techniques are:

- The adjoint-based observation sensitivity measures the impact of observations when the entire observational dataset is present in the assimilation system, while the observing system is modified in

the OSE. In fact, each OSE experiment differs from the others in terms of assimilated observations.

- The adjoint-based technique measures the impact of observations separately at every analysis cycle versus the background, while the OSE measures the total impact of removing data information from both background and analysis.
- The adjoint-based technique measures the response of a single forecast metric to all perturbations of the observing system, while the OSE measures the effect of a single perturbation on all forecast metrics.
- The adjoint-based technique is restricted by the tangent linear assumption and therefore it is valid for forecasts up to 2-days, while the OSE can measure the data impact on longer range forecast and in non linear regimes.

The aim of this paper is to introduce the mathematical concept and the application of the forecast sensitivity to the observation tool. The general ECMWF system performance in the 24 hour range forecast is shown as derived by the diagnostic tool.

In 2, the theoretical background of the FSO and the calculation of the forecast error contribution (FEC) from observations are shown. The ECMWF forecast performance is illustrated in 3 and conclusions are drawn in 4.

2 Observational Impact on the Forecast

(a) Linear analysis equation

Data assimilation systems for numerical weather prediction (NWP) provide estimates of the atmospheric state $\mathbf{x}$ by combining meteorological observations $\mathbf{y}$ with prior (or background) information $\mathbf{x_b}$. A simple Bayesian normal model provides the solution as the posterior expectation for $\mathbf{x}$, given $\mathbf{y}$ and $\mathbf{x_b}$. The same solution can be achieved from a classical *frequentist* approach, based on a statistical linear analysis scheme providing the Best Linear Unbiased Estimate (Talagrand 1997) of $\mathbf{x}$, given $\mathbf{y}$ and $\mathbf{x_b}$. The optimal general least square solution to the analysis problem (see Lorenc 1986) can be written as:

$$\mathbf{x_a} = \mathbf{Ky} + (\mathbf{I} - \mathbf{KH})\mathbf{x_b} \tag{1}$$

The vector $\mathbf{x_a}$ is called the 'analysis'. The gain matrix $\mathbf{K}$ (of dimension $n \times p$ with n being the state vector and p the observation vector dimensions) takes into account the respective accuracies of the background vector $\mathbf{x_b}$ and the observation vector $\mathbf{y}$ as defined by the $(n \times n)$-dimensioned covariance matrix $\mathbf{B}$ and the $(p \times p)$-dimensioned covariance matrix $\mathbf{R}$, with:

$$\mathbf{K} = (\mathbf{B^{-1}} + \mathbf{H^T R^{-1} H})^{-1} \mathbf{H^T R^{-1}} \tag{2}$$

and **I** is the $(n \times n)$ identity matrix. Here, **H** is a $(p \times n)$-dimensioned matrix interpolating the background fields to the observation locations, and transforming the model variables to observed quantities (e.g. radiative transfer calculations transforming the models temperature, humidity, ozone etc. to brightness temperatures as observed by satellite instruments). In the 4D-Var context introduced above, **H** is defined to also include the propagation of the atmospheric state vector by the forecast model to the time at which the observations were recorded.
From (1) the sensitivity of the analysis system with respect to the observations can be derived from:

$$\frac{\delta \mathbf{x_a}}{\delta \mathbf{y}} = \mathbf{K^T} \tag{3}$$

(3) provides the observational influence in the analysis (Cardinali *et al.* 2004).

(b) Sensitivity equation

Baker and Daley (2000) derived the forecast sensitivity equation with respect to the observations in the context of variational data assimilation. Let us consider a scalar J-function of the forecast error. The sensitivity of J with respect to the observations can be obtained using a simple derivative chain as:

$$\frac{\delta J}{\delta \mathbf{y}} = \frac{\delta J}{\delta \mathbf{x_a}} \frac{\delta \mathbf{x_a}}{\delta \mathbf{y}} \tag{4}$$

where $\delta J / \delta \mathbf{x_a}$ is the sensitivity of the forecast error to the initial conditions (Rabier *et al.* 1996, Gelaro *et al.*, 1998). The forecast error is mapped onto the initial conditions by the adjoint of the model providing, for example, regions that are particularly sensitive to forecast error growth (see 2(c)). By using (2) and (3) the forecast sensitivity to the observations becomes:

$$\frac{\delta J}{\delta \mathbf{y}} = \mathbf{K^T} \frac{\delta J}{\delta \mathbf{x_a}} = \mathbf{R^{-1}H}(\mathbf{B^{-1}} + \mathbf{H^T R^{-1} H})^{-1} \frac{\delta J}{\delta \mathbf{x_a}} \tag{5}$$

where $(\mathbf{B^{-1}} + \mathbf{H^T R^{-1} H})^{-1}$ is the analysis error covariance matrix **A**.
In practice, a second-order sensitivity gradient is needed (Langland and Baker, 2004; Errico 2007) to obtain the information related to the forecast error because the first-order sensitivity gradient only contains information on the sub-optimality of the assimilation system (see 2(c) and Cardinali 2009).
The forecast error is defined by $J = 1/2 \langle \mathbf{e}_t, \mathbf{C}\mathbf{e}_t \rangle$ where t stands for the *truth*. **e** denotes the forecast error with respect to temperature, vorticity and divergence as well as surface pressure. In practice, the forecast error is computed as the difference between the 24-hour forecast and the analysis valid at the same time. This implies that the verifying analysis is considered to be the *truth*:

- The verifying analysis is only a proxy of the truth and thus errors in the analysis can obscure the observation impact in the short-range forecast.

C is a matrix of weighting coefficients that integrate the elements of the forecast error to a dry energy norm that is a scalar:

- Energy norm is a suitable choice because it directly depends on the most relevant model parameters also contained in the control vector **x** (the vectors used in the minimization process in e.g 4D-Var). Nevertheless, alternative functions of model parameters can be used.

Equation (5) can be solved (Krylov-method, Van der Vorst 2003) and the forecast error sensitivity to all assimilated observations is then derived. The numerical method used is shown is 2(d) (see also Cardinali 2009)

(c) Sensitivity gradient

Lets consider two forecasts of length f starting from $\mathbf{x}_a$ and length g starting from $\mathbf{x}_b$, being $\mathbf{x}_b$ the background field used in the $\mathbf{x}_a$ analysis. Both forecasts verify at time t. Following Langland and Baker (2004) and Errico (2007) the second-order sensitivity gradient is defined as:

$$\frac{\delta J}{\delta \mathbf{x_a}} = \frac{\delta J_f}{\delta \mathbf{x_a}} + \frac{\delta J_g}{\delta \mathbf{x_b}} \tag{6}$$

Where $J_f = \langle$ **(** $\mathbf{x}_f$ **-** $\mathbf{x}_t$**), C(**$\mathbf{x}_f$ **-** $\mathbf{x}_t$**)** $\rangle$ /2 and $J_g = \langle$ **(** $\mathbf{x}_g$ **-** $\mathbf{x}_t$**), C(**$\mathbf{x}_g$ **-** $\mathbf{x}_t$**)** $\rangle$ /2 are a quadratic measure of the two forecast errors ($\mathbf{x}_t$ the verifying analysis), and **C** is the matrix of dry energy weighting coefficients. It is clear that from (4) the adjoint model maps the sensitivity (with respect to the forecast) of J_f into $\delta J_f / \delta \mathbf{x}_a$ along the trajectory f and the sensitivity of J_g into $\delta J_g / \delta \mathbf{x}_a$ along the trajectory g (see Rabier *et al.* 1996, Gelaro *et al.*, 1998 for the first-order sensitivity gradient definition and computation). Equation (6) is schematically represented

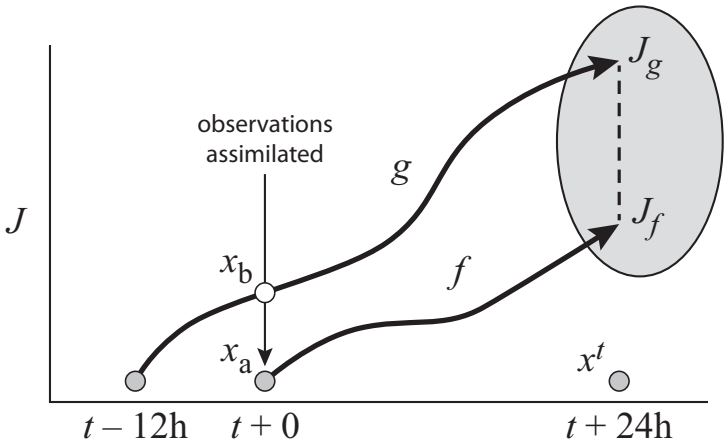

Figure 1: Geometrical representation of the sensitivity gradient calculation expressed in (6).

Lets now compare the first-order sensitivity gradient with the second-order one. Lets define $J_1(\mathbf{e}) = \|\mathbf{e,Ce}\|$, J_1 (**e**), express the variation of the forecast error due to the assimilation of observations, that

is J($\mathbf{e}_a$) - J($\mathbf{e}_b$) where the $\mathbf{e}_a$ and $\mathbf{e}_b$ are the analysis and the background error. Following Langland and Baker, the second-order Taylor series decomposition (see also Errico 2007) is used to map such variation:

$$J(\mathbf{e_b}) - J(\mathbf{e_a}) = (\mathbf{e_b} - \mathbf{e_a})^T J'_{e_a} + \frac{1}{2}(\mathbf{e_b} - \mathbf{e_a})^T J''_{e_a}(\mathbf{e_b} - \mathbf{e_a}) \tag{7}$$

Because the error cost function is quadratic, (7) reduces to

$$J(\mathbf{e_b}) - J(\mathbf{e_a}) = 2(\mathbf{e_b} - \mathbf{e_a})^T \mathbf{e_a} + (\mathbf{e_b} - \mathbf{e_a})^T (\mathbf{e_b} - \mathbf{e_a}) \tag{8}$$

which at the first order is

$$J(\mathbf{e_b}) - J(\mathbf{e_a}) = 2\mathbf{d}^T \mathbf{K}^T \mathbf{e_a} \tag{9}$$

In an optimal assimilation system, the right hand side of the equation is on average zero (Talagrand, 2002) since statistically, the innovation vector, **d=y-Hx**$_b$, and the analysis error are orthogonal. Therefore, it is clear that the results obtained by using the first-order sensitivity gradient, only provides the measure of the sub-optimality of the analysis system. The second-order term appears necessary to be included in the FSO calculation.

(d) Numerical solution

In an optimal variational analysis scheme, the analysis error covariance matrix **A** is approximately the inverse of the matrix of second derivatives (the Hessian) of the analysis cost function $\mathbf{J}_a$ (Rabier *et al.* 2000), i.e. **A=(J**$_a''$**)**$^{-1}$ (Rabier and Courtier 1992). Given the large dimension of the matrices involved, $\mathbf{J}_a''$ and its inverse cannot be computed explicitly. The minimization is performed in terms of a transformed variable χ, χ=**L**$^{-1}$**(x-x**$_b$**)**, with **L** chosen such that **B=LL**^{T} . The transformation **L** thus reduces the covariance of the prior to the identity matrix. In variational data assimilation, **L** is referred to as the change-of-variable operator (Courtier *et al.* 1998). Lets apply the change-of-variable in the analysis cost function and write:

$$\begin{aligned} \mathbf{J_a}(\mathbf{x}) &= \frac{1}{2}(\mathbf{x} - \mathbf{x_b})^T \mathbf{B^{-1}}(\mathbf{x} - \mathbf{x_b}) + \frac{1}{2}(\mathbf{Hx} - \mathbf{y})^\mathbf{T} \mathbf{R^{-1}}(\mathbf{Hx} - \mathbf{y}) \\ &= \frac{1}{2}\chi^\mathbf{T}\chi + \frac{1}{2}(\mathbf{HL}\chi - \mathbf{y})^\mathbf{T}\mathbf{R^{-1}})(\mathbf{HL}\chi - \mathbf{y}) = \mathbf{J_a}(\chi) \end{aligned} \tag{10}$$

The Hessian becomes:

$$\mathbf{J_a}''(\chi) = \mathbf{I} + \mathbf{L^T H^T R^{-1} HL} \tag{11}$$

By applying the change-of-variable in (7) and by using (8), the forecast sensitivity to the observations is expressed as:

$$\frac{\delta J}{\delta \mathbf{y}} = \mathbf{R^{-1} HL}(\mathbf{I} + \mathbf{L^T H^T R^{-1} HL})^{-1} \mathbf{L^T} \frac{\delta J}{\delta \mathbf{x_a}} \tag{12}$$

Using the conjugate gradient algorithm, first the following equation for $\delta J/\delta \mathbf{y} = \mathbf{R^{-1} Hz}$ is solved:

$$\begin{aligned} (\mathbf{I} + \mathbf{L^T H^T R^{-1} HL})\mathbf{z} &= \mathbf{L z_a} \\ \mathbf{z_a} &= \frac{\delta J}{\delta \mathbf{x_a}} \end{aligned} \tag{13}$$

The solution $\mathbf{z}$ lies in the Krylov-subspace generated by the vector $\mathbf{L}^T\mathbf{z}_a$ and the matrix $(\mathbf{I}+\mathbf{L^T H^T R^{-1} HL})$. The Krylov-subspace dimension is the degree of the minimal polynomial of $(\mathbf{I}+\mathbf{L^T H^T R^{-1} HL})$. Therefore if the degree is low, the Krylov-method searches the solution on a small dimensioned space. The method is very efficient in an iterative solution of a linear system with large and sparse matrices (Van der Vorst 2003). The forecast sensitivity to observations is then given by interpolating $\mathbf{z}$ (using the $\mathbf{H}$ operator) in the observation space and by normalizing with respect to the observation error covariance matrix $\mathbf{R}$.

(e) Observation impact measure

Once the forecast sensitivity is computed, the variation δJ of the forecast error expressed by J can be found by rearranging (1) and by using the adjoint property for the linear operator:

$$\begin{aligned}\delta J = \langle \frac{\delta J}{\delta \mathbf{x_a}}, \delta \mathbf{x_a} \rangle &= \langle \frac{\delta J}{\delta \mathbf{x_a}}, \mathbf{K}(\mathbf{y}-\mathbf{Hx_b}) \rangle \\ &= \langle \mathbf{K}^T \frac{\delta J}{\delta \mathbf{x_a}}, \mathbf{y}-\mathbf{Hx_b} \rangle \\ &= \langle \mathbf{K}^T \frac{\delta J}{\delta \mathbf{x_a}}, \delta \mathbf{y} \rangle = \langle \frac{\delta J}{\delta \mathbf{y}}, \delta \mathbf{y} \rangle \end{aligned} \tag{14}$$

where $\delta \mathbf{x_a} = \mathbf{x_a} - \mathbf{x_b}$ are the analysis increments and $\delta \mathbf{y} = \mathbf{y} - \mathbf{Hx_b}$ is the innovation vector. δJ is computed across the 12 hour window; the sensitivity gradients $\delta J / \delta \mathbf{x_a}$, valid at the starting time of the 4D-Var window (09 and 21 UTC in the ECMWF system), are distributed by $\mathbf{K}^T$, which incorporates the temporal dimension, over the 12-hour window. From Eq. (14), few considerations should be taken into account:

- The forecast impact δJ (hereafter called Forecast Error Contribution, FEC) of all observations assimilated depends on the forecast error ($J(\mathbf{e}) \rightarrow \delta \mathbf{J}/\delta \mathbf{x_a}$), the assimilation system ($\mathbf{K}^T$) and the difference between the observations and the model ($\mathbf{y} - \mathbf{Hx_b}$).
- Positive forecast error variation $\delta J > 0$ is synonymous of forecast degradation. Negative forecast error variation $\delta J < 0$ is synonymous of forecast improvement.
- The verifying analysis is only a proxy of the truth. Therefore, errors in the analysis can mask the observation impact in the forecast.
- Biases in the model can result on forecast degradation that erroneously is interpreted as an observation related degradation.
- Since the computation is performed with the linearized model, only errors in the short-range forecast can be diagnosed.
- The forecast error is measured using a dry energy norm that depends on wind, temperature and surface pressure. Therefore, observables depending on these parameters are rather well assessed. Moreover, the dependency of the forecast error on humidity is represented by the linearized moist process so that also forecast impact of humidity observations are fully assessed (Janiskova and Cardinali 2012 in preparation).
- The variation of the forecast error due to a specific measurement can be summed up over time and space in different subsets to compute the average contribution of different components of the

observing system to the forecast error. For example, the contribution of all AMSU-A satellites, *s*, and channels, *i*, over time T will be:

$$\delta J_{AMSU-A} = \sum_{s \subset S} \sum_{i \subset channel} \sum_{t \subset T} = \delta J_{it}^{s}$$

This is one of the most important characteristics of the tool because it allows any necessary level of granularity in analysis for a comprehensive investigation.

Given all the points above it is clear that a full diagnostic assessment is necessary to establish the causes for a forecast error increase.

3 Results

The routinely computed observational impact from the operational ECMWF 4D-Var system (Rabier *et al* 2000; Janiskova *et al*. 2002; Lopez and Moreau, 2005) is shown in Fig. 2 for September and October 2011. At ECMWF, the 'observation impact'-suite runs one day behind the model-suite, in time to recover the actual verifying analysis for the forecast error computation. The 24-hour forecast error contribution (FEC) of all the observing system components is computed and shown in the top panel of Fig. 2 for different observation types as defined in Table 1. Due to technical reasons, microwave imagers (SSMIS and TMI) have not been considered in this study. The largest contribution to decreasing the forecast error is provided by AMSU-A ($\sim$ 25 %), IASI, AIRS, AIREP (aircraft data and GPS-RO observations account for 10% of the total impact, respectively. TEMP and SYNOP surface pressure observations contribute by 5% followed by AMVs and HIRS ($\sim$4%), then by ASCAT and DRIBU (3%). All other observations contribute to less than 3%.

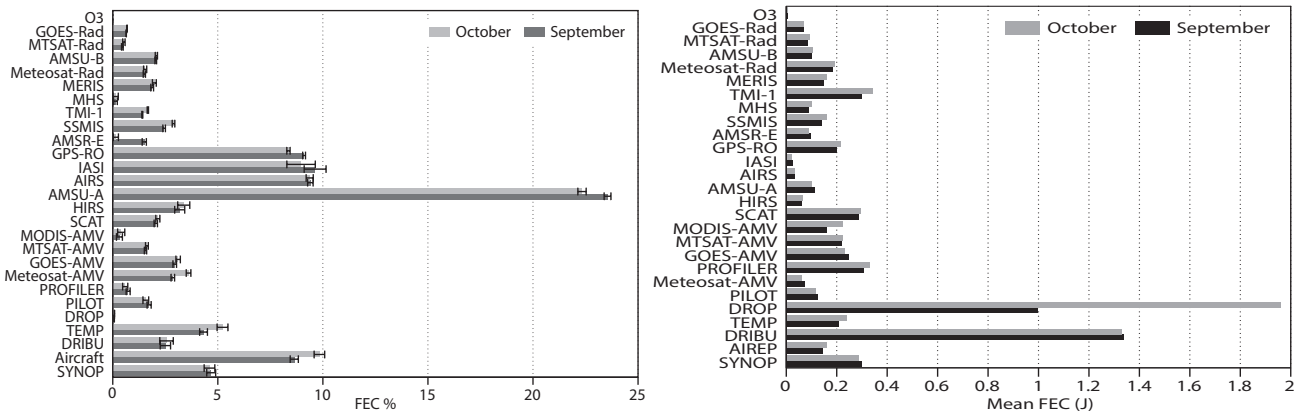

Figure 2: Observation contribution to the global forecast error reduction grouped by observation type as defined in 1. The measure is given in percent and for the months of September and October. Left panel is total forecast error contribution and the error bars are computed using the standard error measure. In the right panel the average forecast error contribution (normalized by the number of observations used) is shown.

The error of the observation impact measure is also displayed in Fig. 2 (top panel) which depend on the standard error and on the number of observation assimilated in that period. If the FEC measures variability is within the error range, the variation is not considered to be significant. In the bottom panel of

Data name	Data kind	Information
OZONE (O3)	Backscattered solar UV radiation, retrievals	Ozone, stratosphere
GOES-Radiance	US geostationary satellite infrared sounder radiances	Moisture, mid/upper troposphere
MTSAT-Rad	Japanese geostationary satellite infrared sounder radiances	Moisture, mid/upper troposphere
MET-rad	EUMETSAT geostationary satellite infrared sounder radiances	Moisture, mid/upper troposphere
AMSU-B	Microwave sounder radiances	Moisture, troposphere
MHS	Microwave sounder radiances	Moisture, troposphere
MERIS	Differential reflected solar radiation, retrievals	Total column water vapour
GPS-RO	GPS radio occultation bending angles	Temperature, surface pressure
IASI	Infrared sounder radiances	Temperature, moisture, ozone
AIRS	Infrared sounder radiances	Temperature, moisture, ozone
AMSU-A	Microwave sounder radiances	Temperature
HIRS	Infrared sounder radiances	Temperature, moisture, ozone
ASCAT	Microwave scatterometer backscatter coefficients	Surface wind
MODIS-AMV	US polar Atmospheric Motion Vectors, retrievals	Wind, troposphere
Meteosat-AMV	EUMETSAT geostationary Atmospheric Motion Vectors, retrievals	Wind, troposphere
MTSAT-AMV	Japanese geostationary Atmospheric Motion Vectors, retrievals	Wind, troposphere
GOES-AMV	US geostationary Atmospheric Motion Vectors, retrievals	Wind, troposphere
PROFILER	American, European and Japanese Wind profiles	Wind, troposphere
PILOT	Radiosondes at significant level from land stations	Wind, troposphere
DROP	Dropsondes from aircrafts	Wind, temperature, moisture, pressure, troposphere
TEMP	Radiosondes from land and ships	Wind, temperature, moisture, pressure, troposphere
AIREP	Aircraft measurements	Wind, temperature, troposphere
DRIBU	Drifting buoys	Surface pressure, temperature, moisture, wind
SYNOP	Surface Observations at land stations and on ships	Surface pressure, temperature, moisture, wind

Table 1: Observation type assimilated in September and October 2011. Number of observations per assimilation cycle is $\sim 5\ 10^6$.

Fig. 2, the mean impact per individual observation is shown. In this case, the impact is independent from the observation number. The largest mean contribution is provided by DROP and DRIBU (surface pressure) observations, followed by the contribution of a second group of observations comprising MERIS, AMVs, ASCAT, GPS-RO, SYNOP, TEMP, AMSU-B and AIREP. Contrary to the total forecast impact that is largely provided by satellite observations, the largest per-observation impact is obtained from conventional observations. The difference between the two impact measures is mainly due to difference in observation accuracy through which a single conventional observation is on average more influential in the analysis than a single satellite measurement.

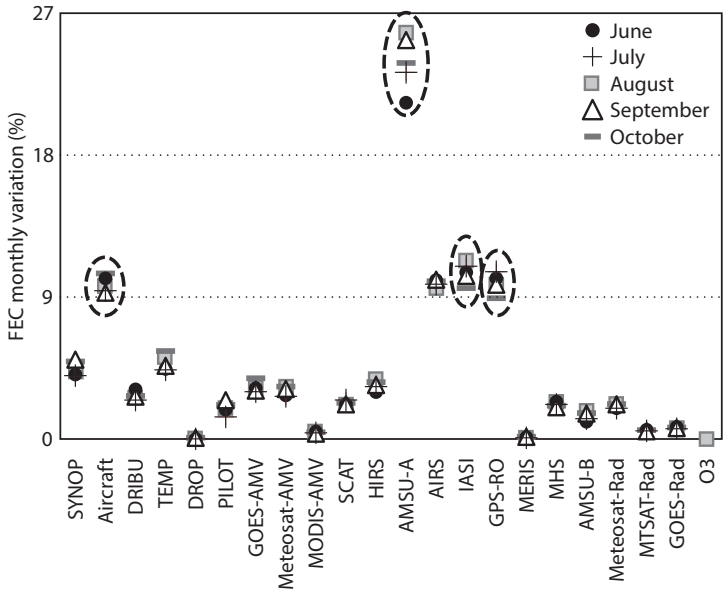

Figure 3: Variation of total Forecast Error Contribution in June, July, August, September and October 2011 for the different observation types.

The monthly variation of forecast impact is shown in Fig. 3 per observation type and for June -October 2011. The only significant temporal variation is observed for AMSU-A with the largest forecast impact in August and September, and for GPS-RO and IASI in July and August, respectively.

The AMSU-A forecast impact has been analyzed in more detail. In 4 the contribution of all channels to the forecast error decrease is shown. Channel 8 has the largest overall impact and the stratospheric channels (11-14) the smallest. There is no significant difference in performance between September and October. The geographical distribution of mean forecast improvement or deterioration from channel 8 is shown in Fig. 5 for September-October 2011. The METOP-A AMSU-A performance is compared with that of NOAA-15 since they have a similar satellite orbit; nevertheless, there is a difference in the measurement time since METOP-A crosses the equator at around 9:30 and NOAA-15 at 16:30. The overall impact of the instrument on the two satellites is comparable. The geographical location of the improvement instead differs quite substantially with the exception of the polar and central Southern Hemisphere regions where both are performing similarly well. In the western part of the Southern Hemisphere, METOP-A reduces the forecast error whilst NOAA-15 increases it; on the contrary, in the eastern part, NOAA-15 shows a large and consistent improvement whereas METOP-A shows small areas

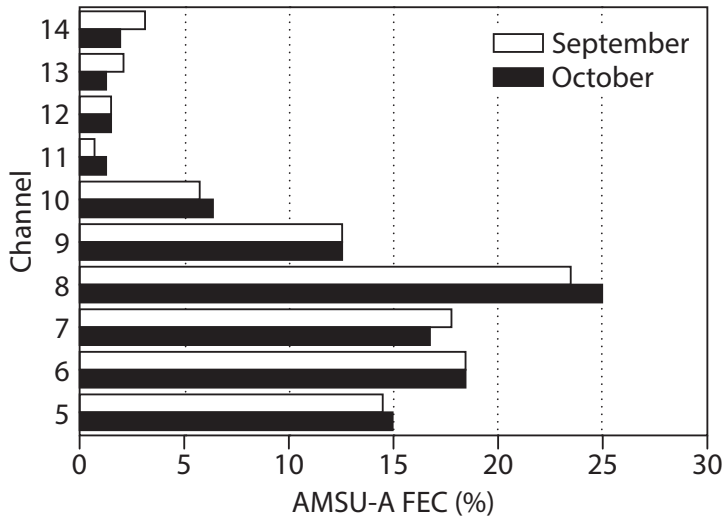

Figure 4: Total Forecast Error Contribution for all AMSU-A instruments in percent. The impact is shown for all assimilated channels and for September and October 2011.

of degradation. A similar impact pattern is observed for the Tropics and Northern Hemisphere.

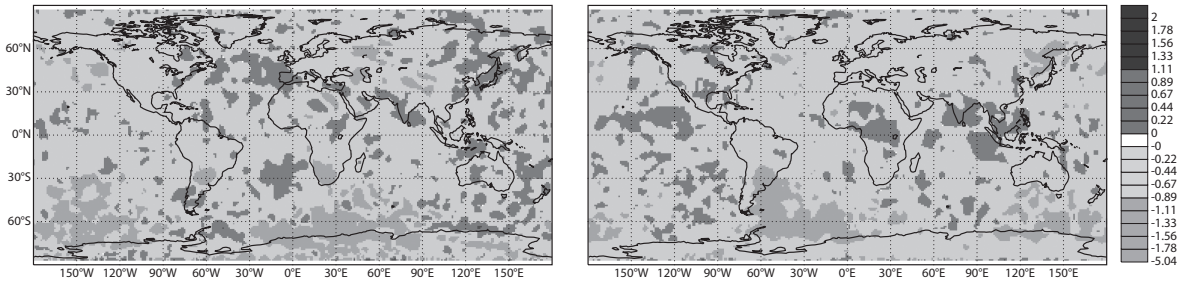

Figure 5: Mean Forecast Error Contribution for AMSU-A channel 8 onboard METOP-A (left panel) and NOAA-15 (right) for the whole globe. Unit is Joule.

Once the area of degradation or improvement and the periods of interest are determined, the addition of OSEs can help to determine the possible causes. For example, can be necessary to identify the explicit contribution of AMSU-A channel 8 to the degradation over the Atlantic (METOP-A) or central Africa (NOAA-15). The comparison between the experiment where channel 8 is not assimilated and the control experiment (in which it s assimilated) will add information for the specific case and will help in evaluating suitability of the assimilation procedure for this data.

The variation of forecast impact with time for AMSU-A channel 8 is shown for the North Atlantic region in Fig. 6 (top panel). Again METOP-A (left panel) and NOAA-15 (right panel) are compared. METOP-A shows much larger temporal variability than NOAA-15 and displays more events of detri-

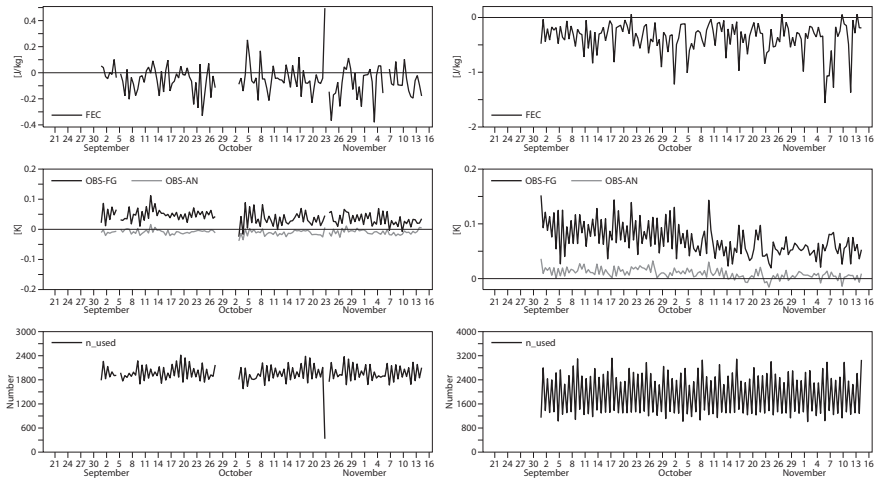

Figure 6: Daily variation of mean FEC (top panel), background (black line) and analysis (grey line) departure (middle panel) and observation number (bottom panel) over the Atlantic region from September to mid November 2011 for METOP-A (left panel) and NOAA-15 (right panel) AMSU-A channel 8.

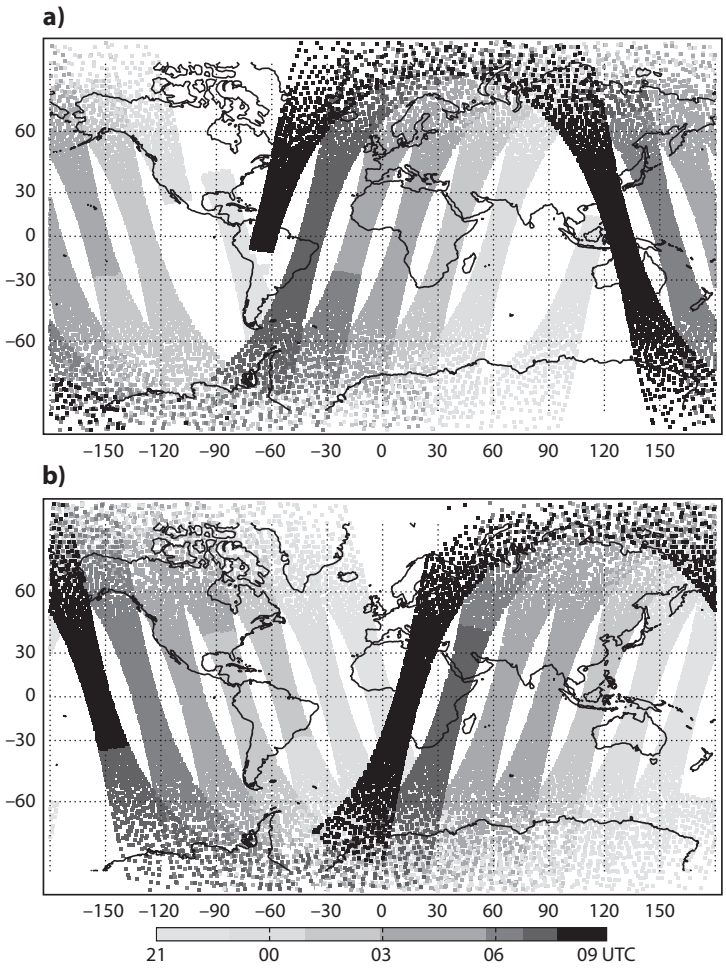

Figure 7: Data coverage for METOP-A (top panel) and NOAA-15 (bottom panel) AMSU-A. The swath colour is related to the measurement time from 21 UTC to 9 UTC.

mental impact (positive values) than NOAA-15 that, except for a few occasions, performs rather well over the entire period. The observation departures are also different: the departures with respect to the background (black line middle panel) is smaller for METOP-A (on average 0.05 K) until the beginning of October when the assimilation of METOP-A restarted after a break of three days due to routine satellite maintenance. After the 2^{nd} of October, METOP-A background departures become smaller but the largest absolute decrease (0.025 K) is observed instead for NOAA-15. And, from October onwards, the observation departure from the analysis (grey line middle panel) becomes very similar (close to zero on average) while before that day, NOAA-15 shows a small positive bias. Interestingly, the forecast reduction also changes: METOP-A shows larger variability than before and to a less extent also NOAA-15. However, on average, as shown in Fig. 5, the impact of the two satellites is quantitatively similar though different in terms of location. Over the Pacific, for example, METOP-A and NOAA-15 time series of the forecast performance are more similar, with METOP-A showing also few large improvements (not shown). The number of measurements provided by the two satellites is very similar (bottom panel). The larger forecast error reduction of NOAA-15 with respect to METOP-A over the North Atlantic is due to the measurement time (Fig. 7). In fact, NOAA-15 satellite cross the Atlantic close to 9 UTC which corresponds to the end of the 12 hour assimilation window in the 4D-Var system used (Fig. 7 light grey) whilst the METOP-A platform is observing the Atlantic at the beginning of the assimilation window (Fig. 7 dark grey). Due to the evolution of the model error covariance matrix **B** across the assimilation window, observations assimilated towards the end of the window are more influential than observations assimilated at the beginning of the window.

4 Conclusion

Over the last few years, the potential of using derived adjoint-based diagnostic tools has been largely exploited. Recently, a compact derivation of the 4D-Var sensitivity equations by using the theoretical framework of the implicit function has been derived (Daescu 2008). The analytical formulation of the sensitivity equations with respect to an extended set of input parameters has been shown and numerical applications will soon follow. This paper illustrates the use of the forecast sensitivity with respect to time-distributed observational data, first time in a 12-hour 4D-Var assimilation system, as a diagnostic tool to monitor the observation performance in the short-range forecast. The fundamental principles, on which the forecast sensitivity diagnostic tool is based, are illustrated and an example of a routine diagnostic is provided.

The forecast sensitivity to observations can only be used to diagnose the impact on the short-range forecast, namely for periods of 24 to 48 hours, given the use of the adjoint model and the implied linearity assumption. The tool allows the computation and visualization of the impact for each assimilated measurement and therefore the diagnostic can be performed from local to global scales and for any period of interest. The use the second-order sensitivity gradient is necessary to identify the forecast impact of the observations; in fact, the projected first-order sensitivity gradient only contains information on the suboptimality of the assimilation system. The tools characteristics have been explained: in particular, the dependency of the tool on the verifying analysis used to compute the forecast error and the dependency of the sensitivity tool on the scalar function representing the global forecast error (energy norm). The function of the global forecast error is first mapped onto the initial conditions (using the adjoint operator of the model forecast) and then into the observation space (using the adjoint operator of the analysis system). The forecast error sensitivity of a specific measurement is transformed on forecast error variation

via a scalar product with the innovation vector.

The global impact of observations is found to be positive and the forecast errors decrease for all data type when monthly averaged. In fact, due to statistical nature of the assimilation procedure, the observation impact must be averaged over a long enough period to be significant.

An example of observation impact monitoring has been shown and from the global performance assessment the specific performance of one AMSU-A channel has been illustrated for two polar orbiting satellites, namely METOP-A and NOAA-15 covering a similar orbit. The causes of degradation or improvement can be further investigated using Observing System Experiments.

Given the dependency of some observation types on the meteorological situation, it is suggested to run the forecast sensitivity to the observation diagnostic tool on an operational basis and in relation to the operational suite error. A constant monitoring of the performance of the model forecast would allow the use of the observation network in an adaptive way where observations with negative impact can be investigated and potentially denied in real time.

Acknowledgements

The author thanks Mohamed Dahoui, Anne Fouilloux and Fernando Prates for their continued support to monitor, display and diagnose the forecast performance of all observations assimilated at ECMWF.

References

Baker N.L. and R. Daley, 2000: Observation and background adjoint sensitivity in the adaptive observation targeting problem. Q. J. R. *Meteorol. Soc,* **126**,1431-1454

Bouttier, F, and Kelly, G., 2001: Observing system experiments in the ECMWF 4D-Var data assimilation system. Q. J. R. *Meteorol . Soc*, **127**,1469-1488

Cardinali, C., S. Pezzulli and E. Andersson, 2004: Influence matrix diagnostics of a data assimilation system. Q. J. R. *Meteorol. Soc*, **130**, 2767-2786

Cardinali, C., and R. Buizza, 2004. Observation sensitivity to the analysis and the forecast: a case study during ATreC targeting campaign. Proceedings of the First THORPEX International Science Symposium, 6-10 December 2004, Montreal, Canada, WMO TD 1237 WWRP/THORPEX N. 6.

Cardinali, C., 2009: Monitoring the observation impact on the short-range forecast. Q. J. R. *Meteorol. Soc.*, **135**, 239-250

Chapnik, B., G.Desnrozier, F. Rabier and O. Talagrand, 2006: Diagnosis and tuning of observation error

in a quasi-operational data assimilation setting. Q. J. R. *Meteorol. Soc.*, **132**, 543-565.

Courtier P., E. Andersson, W. Heckley, J. Pailleux, D. Vasiljevic, M. Hamrud, A. Hollingsworth, F. Rabier and M. Fisher, 1998: The ECMWF implementation of three-dimension variational assimilation (3D-Var). Part I: Formulation. Q. J. R. *Meteorol. Soc.*, **124**, 1783-1807

Daescu, D.N., 2008: On the sensitivity equations of 4D-Var data assimilation. *Mon. Wea. Rev.*, accepted for publication.

English, S., R. Saunders, B. Candy, M. Forsythe, and A. Collard, 2004: Met Office satellite data OSEs. Third WMO Workshop on the impact of various observing systems on numerical weather prediction, Alpbach, Austria, WMO/TD, **1228**, 146-156

Errico, R., 2007: Interpretation of an adjoint-derived observational impact measure. *Tellus*, **59A**, 273-276.

Gelaro R, Buizza, R., Palmer T.N. and Klinker E., 1998: Sensitivity analysis of forecast errors and the construction of optimal perturbations using singular vectors. *J. Atmos. Sci.*, **55**, 1012-1037.

Kelly, G., 2007: Evaluation of the impact of the space component of the Global Observation System through Observing System Experiments. ECMWF Newsletter Autumn.

Langland R. and N.L Baker., 2004: Estimation of observation impact using the NRL atmospheric variational data assimilation adjoint system. *Tellus*, **56A**, 189-201.

Lorenc, A., 1986: Analysis methods for numerical weather prediction. *Q. J. R. Meteorol. Soc.*, **112**, 1177-1194.

Lopez, P. and E. Moreau, 2005: A convection scheme for data assimilation: Description and initial tests. *Q.J.R.Meteorol.Soc.*, **131**, 409-436

Lord, S., T. Zapotocny, and J. Jung, 2004: Observing system experiments with NCEPs global forecast system.Third WMO Workshop on the impact of various observing systems on numerical weather prediction, Alpbach, Austria, WMO/TD, **1228**, 56-62.

Lupu, C., P. Gauthier and S. Laroche, 2011: Evaluation of the impact of observations on analyses in 3D- and 4D-Var based on information content. *Mon. Wea. Rev.*, **139**, 726-737.

Janiskova, M., J.-J. M. J.-F. Mahfouf, and F. Chevallier, 2002: Linearized radiation and cloud schemes in the ECMWF model: Development and evaluation, *Q. J. R. Meteorol. Soc.*, **128**, 1505-1527.

Rabier, F. and Courtier, P., 1992: Four-dimensional assimilation in the presence of baroclinic instability. *Q. J. R. Meteorol. Soc.*, **118**, 649-672.

Rabier, F., Klinker, E., Courtier, P. and Hollingsworth A. 1996: Sensitivity of forecast errors to initial condition. *Q. J. R. Meteorol. Soc.* **122**, 121-150

Rabier, F., Jrvinen, H., Klinker, E., Mahfouf J.F., and Simmons, A., 2000: The ECMWF operational implementation of four-dimensional variational assimilation. Part I: experimental results with simplified physics. *Q. J. R. Meteorol. Soc.* **126**, 1143-1170.

Radnoti, G., P. Bauer, A. P. McNally, C. Cardinali, S. Healy and P. deRosnay, 2010: ECMWF study on the impact of future developments of the space-based observing system on Numerical Weather Prediction. ECMWF Technical Memorandum, No. 638, 117 pp. Available from European Centre for Medium-Range Weather Forecasts, Shinfield Park, Reading RG2 9AX, United Kingdom.

Radnoti, G., P. Bauer, A. P. McNally and A. Horanyi, 2012: ECMWF study to quantify the interaction between terrestrial and space-based observing systems on Numerical Weather Prediction skill. Project report, available from ECMWF.

Talagrand, O., 1997: Assimilation of observations, an Introduction. *J. Meteorol. Soc. Japan*, **Vol 75**, N.1B,191-209.

Talagrand O., 2002: A posteriori validation of assimilation algorithms. Proceding of NATO Advanced Study Institute on Data Assimilation for the Earth System, Acquafreda, Maratea, Italy.

Tompkins, A.M. and M. Janiskova: 2004, A cloud scheme for data assimilation: Description and initial tests. *Q.J.R.Meteorol.Soc*, **130**, 2495-2517

Van der Vorst, H.A., 2003: Iterative Krylov methods for large linear systems. *Cambridge Accademic Press*

Zhu, Y. and Gelaro, R., 2008: Observation Sensitivity Calculations Using the Adjoint of the Gridpoint Statistical Interpolation (GSI) Analysis System. *Mon. Wea. Rev.*, **136**, 335-351.